A peer-reviewed version of this preprint was published in PeerJ on 1 March 2018.

View the peer-reviewed version (peerj.com/articles/4449), which is the preferred citable publication unless you specifically need to cite this preprint.

Brüwer JD, Voolstra CR. 2018. First insight into the viral community of the cnidarian model metaorganism Aiptasia using RNA-Seq data. PeerJ 6:e4449 https://doi.org/10.7717/peerj.4449

Insights into viral community composition of the cnidarian model metaorganism Aiptasia using RNA-Seq data

Jan D Brüwer [1] , **Christian Voolstra** Corresp. [1]

[1] Red Sea Research Center, King Abdullah University of Science and Technology

Corresponding Author: Christian Voolstra
Email address: christian.voolstra@kaust.edu.sa

Current research posits that all multicellular organisms live in symbioses with associated microorganisms and form so-called metaorganisms or holobionts. Cnidarian metaorganisms are of specific interest given that stony corals provide the foundation of the globally threatened coral reef ecosystems and their well-being strongly relies on forming mutualistic relationships with endosymbiotic algae of the genus *Symbiodinium*. So far, only few studies characterized viral diversity and the potential underlying functional importance to coral holobionts. Here we analyzed an existing RNA-Seq dataset of the coral model metaorganism Aiptasia CC7 (*sensu Exaiptasia pallida*) associated with aposymbiotic, partially populated, and fully symbiotic anemones with *Symbiodinium* to gain further insight into viral community composition and the relation to the algal endosymbiosis. Our approach included the selective removal of anemone host and algal endosymbiont sequences and subsequent microbial sequence annotation. Of a total of 297 million raw sequence reads, 8.6 million (~ 3%) remained after host and endosymbiont sequence removal. Of these, 3,293 sequences (paired-end read pairs) could be assigned as of viral origin. Taxonomic annotation shows that Aiptasia is associated with a diverse viral community consisting of 116 viral taxa covering 40 families. The viral community was dominated by viruses from the families *Herpesviridae* (12.00%), *Partitiviridae* (9.93%), and *Picornaviridae* (9.87%). Despite an overall stable viral community, we found that some viral taxa significantly changed in relative abundance when Aiptasia engage in a symbiotic relationship with *Symbiodinium*. Elucidation of viral taxa consistently present in all samples revealed an Aiptasia core virome of 15 viral taxa from 11 viral families that was comprised of many viruses previously reported in coral viromes. Our study provides a first insight into the viral community of Aiptasia. Aiptasia seem to harbor a diverse and overall stable viral community, although certain members change in abundance when the anemone host associates with its algal endosymbiont. However, the functional significance of this remains to be determined.

Insights into viral community composition of the cnidarian model metaorganism Aiptasia using RNA-Seq data

Jan D Brüwer[1], Christian R Voolstra[1*]

Author Affiliations

[1]Red Sea Research Center, Division of Biological and Environmental Science and Engineering (BESE), King Abdullah University of Science and Technology (KAUST), Thuwal 23955-6900, Saudi Arabia

* Corresponding Author

Email: Christian.voolstra@kaust.edu.sa

Phone: +966 54 470 0087

Fax: +966 21 8082377

Short title

Viral community of Aiptasia CC7

Keywords

Model organism, Aiptasia*, Exaiptasia pallida,* virus, RNA-Seq, metaorganism, holobiont, symbiosis

Abstract

Current research posits that all multicellular organisms live in symbioses with associated microorganisms and form so-called metaorganisms or holobionts. Cnidarian metaorganisms are of specific interest given that stony corals provide the foundation of the globally threatened coral reef ecosystems and their well-being strongly relies on forming mutualistic relationships with endosymbiotic algae of the genus *Symbiodinium*. So far, only few studies characterized viral diversity and the potential underlying functional importance to coral holobionts. Here we analyzed an existing RNA-Seq dataset of the coral model metaorganism Aiptasia CC7 (*sensu Exaiptasia pallida*) associated with aposymbiotic, partially populated, and fully symbiotic anemones with *Symbiodinium* to gain further insight into viral community composition and the relation to the algal endosymbiosis. Our approach included the selective removal of anemone host and algal endosymbiont sequences and subsequent microbial sequence annotation. Of a total of 297 million raw sequence reads, 8.6 million (~ 3%) remained after host and endosymbiont sequence removal. Of these, 3,293 sequences (paired-end read pairs) could be assigned as of viral origin. Taxonomic annotation shows that Aiptasia is associated with a diverse viral community consisting of 116 viral taxa covering 40 families. The viral community was dominated by viruses from the families *Herpesviridae* (12.00%), *Partitiviridae* (9.93%), and *Picornaviridae* (9.87%). Despite an overall stable viral community, we found that some viral taxa significantly changed in relative abundance when Aiptasia engage in a symbiotic relationship with *Symbiodinium*. Elucidation of viral taxa consistently present in all samples revealed an Aiptasia core virome of 15 viral taxa from 11 viral families that was comprised of many viruses previously reported in coral viromes. Our study provides a first insight into the viral community of Aiptasia. Aiptasia seem to harbor a diverse and overall stable viral community, although certain members change in abundance when the anemone host associates with its algal endosymbiont. However, the functional significance of this remains to be determined.

Introduction

Research in the last few decades support the notion that multicellular organisms do not live in isolation, but are forming complex relationships with a variety of microorganisms including bacteria, archaea, and viruses (McFall-Ngai et al., 2013). This entity of host organism and microorganisms is termed 'metaorganism' or 'holobiont' (Rohwer et al., 2002; Knowlton & Rohwer, 2003; Bosch & McFall-Ngai, 2011). Among invertebrate animal hosts, stony corals form holobionts of particular interest given they engage in endosymbioses with photosynthetic algae of the genus *Symbiodinium* that form the basis of coral reef ecosystems and are of high economic and ecologic importance (Muscatine & Porter, 1977; Hoegh-Guldberg, 1999). While the cnidarian host provides a light-rich but sheltered environment, *Symbiodinium* supply energy-rich sugars in the form of photosynthates (Muscatine, 1967; Falkowski et al., 1984). In turn, the associated bacterial community provides functions important for nutrient cycling (Lesser & Jarett, 2014; Rädecker et al., 2015), pathogen defense and immune system, and potentially stress resilience (Rosenberg et al., 2007; Torda et al., 2017; Ziegler et al., 2017). The importance of the viral community has become more recently the focus of research. However, the functional importance is not entirely clear, although recent studies suggest that viruses play a role in some coral diseases and potentially coral bleaching (Marhaver, Edwards & Rohwer, 2008; Soffer et al., 2014; Weynberg et al., 2015, 2017; Correa et al., 2016; Levin et al., 2016; Brüwer et al., 2017; Vega Thurber et al., 2017).

Unfortunately, corals are under increasing threat from anthropogenic influences, in particular climate change (Hoegh-Guldberg, 1999; Hughes et al., 2003, 2017; IPCC, 2014), and understanding coral metaorganisms is critical in order to mitigate strategies to conserve coral reef ecosystems. To this end, the sea anemone Aiptasia (*sensu Exaiptasia pallida*) is becoming a popular model system to investigate the coral-dinoflagellate symbiosis (Weis et al., 2008; Voolstra, 2013; Baumgarten et al., 2015). While some studies looked into the association of Aiptasia with *Symbiodinium* (Thornhill et al., 2013; Xiang et al., 2013; Hambleton, Guse &

Pringle, 2014; Wolfowicz et al., 2016) and bacteria (Röthig et al., 2016; Herrera et al., 2017), the viral community composition, to our knowledge, has not yet been investigated.

To provide a first insight into viral community composition of the cnidarian model system Aiptasia, we employed a strategy used by Brüwer et al. (2017) to re-analyze a previously published RNA-Seq dataset (Baumgarten et al., 2015). The transcriptomic data comprised aposymbiotic Aiptasia as well as anemones partially populated and fully symbiotic with endosymbiotic algae of *Symbiodinium minutum* (strain SSB01, Clade B1). Our strategy entailed the removal of anemone host and algal endosymbiont sequences and subsequent taxonomic annotation of remaining sequences to assess viral community composition and also to determine whether the symbiotic state potentially influences viral association.

Material & Methods

We used a previously published RNA-Seq dataset (NCBI accessions: SRX757525 - adult, aposymbiotic Aiptasia CC7, 4 replicates; SRX757526 - adult Aiptasia CC7 partially populated with *Symbiodinium minutum*, 4 replicates; SRX757528 – adult Aiptasia CC7 fully symbiotic with *Symbiodinium minutum*, 4 replicates) of Aiptasia strain CC7 (*sensu Exaiptasia pallida*) generated for the purpose of assembling a reference transcriptome for the Aiptasia CC7 genome (Baumgarten et al., 2015). Animal culturing, experimental treatments, RNA extraction, and sequencing are briefly outlined below and reported in detail in Baumgarten et al. (2015).

Culturing of Aiptasia anemones and experimental treatments

Anemones of the clonal Aiptasia strain CC7 were kept in a circulating artificial seawater system at the following rearing conditions: ~25°C with 20-40 µmol photons m^{-2} s^{-1} photosynthetically active radiation on a 12 h:12 h light:dark cycle. They were fed freshly hatched *Artemia salina* nauplii twice per week. In order to generate aposymbiotic anemones (i.e., without dinoflagellate symbionts), anemones were repeatedly treated with a cold-shock by transferring for 4h to 4°C water and subsequent exposure to the photosynthesis inhibitor diuron (Sigma-Aldrich #D2425) at 50 µM. The anemones were maintained for ≥1 month in the above-detailed rearing conditions to assure no repopulation by any residual dinoflagellates. Before further treatments were applied, anemones were inspected individually via fluorescence stereomicroscopy to confirm absence of *Symbiodinium*. To generate, partially populated and fully symbiotic anemones, animals were kept in autoclaved and sterile-filtered artificial seawater (AFSW; other conditions as described above) and were infected with *Symbiodinium minutum* (strain SSB01, clade B1): day 1, algae were added at ~10^5 cells/ml; day 2, brine shrimp were added without a water change or addition of algae; day 3, AFSW was changed and algae added at ~10^5 cells/ml; day 11, the AFSW was changed. Samples were taken at the mid-point of the 12-h light period on day 0 (aposymbiotic), day 12 (partially populated), and day 30 (fully symbiotic).

RNA extraction and sequencing

Total RNA was extracted from the aposymbiotic, partially populated, and fully symbiotic anemones (see above) using TRIzol (Life Technologies #15596-026) following the manufacturer's instructions. The mRNA was extracted from total RNA using Dynabeads oligo$(dT)_{25}$ (Ambion #61002). The quantity and quality were assessed and monitored using a Bioanalyzer 2100 (Agilent Technologies, RNA Nano/Pico Chip). Subsequent library preparations were conducted using the NEBNext Ultra Directional RNA Library Prep Kit (NEB #E7420) with a 180-bp insert size. Libraries were sequenced together on one lane of an Illumina HiSeq2000 sequencer with read lengths of 2 x 101 bp.

Sequence data filtering

The software trimmomatic (Bolger, Lohse & Usadel, 2014) was used for quality control and read trimming (settings: LEADING:30 TRAILING:30 SLIDINGWINDOW:4:30 MINLEN:35 HEADCROP:6 -phred33). Single reads of paired-end read pairs resulting from quality control (see above) were discarded and not considered for downstream analyses. Sequencing adapters were removed with fastq-mcf (Aronesty, 2011) (settings: -l 35 --qual-mean 25). The BBsplit script from BBmap v35 (Bushnell, 2016) was utilized to remove sequencing library spiked-in PhiX174 Illumina control sequences (NCBI accession: NC_001422.1), sequences mapping to the genomes of Aiptasia CC7 (NCBI accession: GCA_001417965.1) (Baumgarten et al., 2015; Liew, Aranda & Voolstra, 2016) and *Symbiodinium minutum* (NCBI accession: GCA_000507305.1) (Shoguchi et al., 2013), as well as any sequences of 28S rRNA of sea anemones from the NCBI 'nr' database (16.03.2017; search term: "(((28S) AND "cnidarians"[porgn:__txid6073]) AND "anthozoans" [porgn:__txid6101]) AND "sea anemones" [porgn:__txid6103])") (settings: minid = 0.7 local = t qin = 33). The reason for the 28S rRNA removal lies in their apparent similarity to two Baculoviridae, namely *Choristoneura occidentalis granulovirus* (ChocGV; CLARK taxonomic id: 364745) and *Chrysodeixis chalcites nucleopolyhedrovirus* (CLARK taxonomic id: 320432). Retained sequence reads were used for all subsequent analyses. Overview of filters applied and commands used are available as Supplementary Information (Supp. Fig. S1, Supp. Data Sheet S1).

Viral community analysis

Of the retained sequence reads (see above) only paired reads were considered and annotated to the highest possible phylogenetic level using the classify_metagenome.sh script of CLARK (Ounit et al., 2015) (settings: -m 0; remaining settings: default) using NCBI's RefSeq database for bacteria, archaea, and viruses. The database was downloaded using the implemented set_target.sh script (version 1.2.3; default settings; RefSeq release 81). Prior to normalization viruses that were only annotated with one sequence in one sample (i.e., singletons) as well as read pairs annotating to *Choristoneura occidentalis granulovirus* (ChocGV) (NCBI id: NC_008168.1; CLARK taxonomic id: 364745) were removed due to similarity to 28S rRNA of sea anemones (see above). For normalization, retrieved raw counts (including bacteria, archaea, and viruses) were normalized using the cumulative-sum scaling (CSS) method implemented in the R Bioconductor package metagenomeSeq (v 1.17.0) (Gentleman et al., 2004; Paulson et al., 2013; Paulson, 2014; R Core Team, 2016), and we subsequently only considered sequences that were classified as of viral origin. Information on diverse groups of viruses (i.e., single strand positive sense RNA ssRNA(+), single strand negative sense RNA ssRNA(-), double strand DNA dsDNA, double strand RNA dsRNA, reverse transcribing RNA ssRNA(rt) as well as known virus hosts (bacteria, fungi, invertebrate, vertebrate, plant, protozoan) were retrieved from either the ICTV website at http://talk.ictvonline.org (Davison, 2017) or ViralZone at http://viralzone.expasy.org (Hulo et al., 2011). Species richness, evenness, and Shannon-Wiener Index (alpha diversity) were estimated using the R package vegan (v. 2.4 – 2) (Oksanen et al., 2017). The R package ggplot2 was used for visualizing the relative abundance of viral taxa and viral families (Wickham, 2016). Overview of viral community analysis and commands used are available as Supplementary Information (Supp. Fig. S1, Supp. Data Sheet S1).

In order to test for statistical differences in the viral community composition of aposymbiotic, partially populated, and fully symbiotic Aiptasia, we conducted analysis of variance (ANOVA) on Pielou's evenness and Shannon-Wiener diversity. Further, we tested for significant differences in relative abundance of viral taxa across conditions. To do this, we

tested viral taxa (n = 116) with an ANOVA and a posthoc Tukey test (R Core Team, 2016) using $p < 0.05$ as a cutoff.

To determine viromes associated with aposymbiotic, partially populated, and fully symbiotic Aiptasia, we determined all viral taxa that were 100% present across all four replicates of the respective condition. Those viral taxa that were present in 100% of all aposymbiotic, partially populated, and fully symbiotic Aiptasia samples were considered to be core virome members. The different viromes, including the core virome, were visualized in a venn diagram using BioVenn (Hulsen, de Vlieg & Alkema, 2008).

Results

Viral sequence annotation

A total of 297,207,704 sequence reads (i.e., 148,603,852 paired-end read pairs) detailing four replicates of adult Aiptasia anemones across each of three symbiotic stages (aposymbiotic, partially populated, and fully symbiotic), i.e. total of 12 samples were available for viral sequence annotation (Table 1, Supp. Fig. S1). Of those, 262,252,332 (88.24%) sequence reads were retained after quality control, read trimming, and adapter removal. After removal of anemone host, algal endosymbionts, and miscellaneous other sequences (see Methods), 8,597,604 (2.89%) sequence reads were available and used for bacterial, archaeal, and viral annotation using the CLARK classification tool (Ounit et al., 2015). A total of 38,090 CLARK classified sequences were retrieved, of which 90.97% (34,649 sequences) were of bacterial, a smaller fraction of only 0.39% (148 sequences) of archaeal, and 8.65% (3,293 sequences) of viral origin. The virus-classified sequences comprised 116 distinct taxa covering 40 viral families (Supp. Table S1).

Aiptasia viral community composition

Aiptasia was associated with a diverse viral community featuring an average species richness of 36.72 (SD ±2.98) following Hurlbert (1971). The viral community was evenly distributed as highlighted by an average Pielou's evenness of 0.90 (SD ±0.02) and Shannon-Wiener diversity was 3.75 (SD ±0.17) across samples (Table 2). Measures of community composition were stable across aposymbiotic, partially populated, and fully symbiotic anemones, as neither Pielou's evenness ($p > 0.88$) nor Shannon-Wiener diversity ($p > 0.50$) were significantly different between different symbiotic states. Almost half of the viral community was encompassed by ssRNA(+) viruses, about a third were annotated as dsDNA viruses, and less than a fifth of the community was comprised by dsRNA viruses. Conversely, ssRNA(-) and ssRNA(rt) were detected at very low frequencies. The ten most abundant viral families accounted for about two-thirds of the viral community (Fig. 1). The most abundant viral families included the *Herpesviridae* (12.00% ± 0.49%), *Partitiviridae* (9.93% ± 0.30%), and *Picornaviridae* (9.87% ± 0.45%). Generally,

212 the community comprised few abundant and many rare viral species across treatments (Fig. 2).
213 The most abundant viral taxon, *Dulcamara mottle virus* (7.16% ± 0.41%), is a vertebrate virus of
214 the *Tymoviridae* family and belongs to the fourth most abundant viral family. The next most
215 abundant viral taxa were *Caviid betaherpesvirus* 2 (6.48% ± 0.29%), *Murid betaherpesvirus* 8
216 (4.34% ± 0.28%), *Jingmen tick virus* (4.31% ± 0.22%), and *Bidens mottle virus* (4.15% ± 0.23%).
217
218 *Viral communities of fully symbiotic Aiptasia are different from aposymbiotic and partially*
219 *populated sea anemones*
220 Despite the overall similarities in viral community composition, we were interested to assess
221 whether some viral taxa were differentially abundant between symbiotic states/conditions.
222 Assessing viral taxon abundance from aposymbiotic to partially populated to fully symbiotic
223 Aiptasia revealed two general patterns (Supp. Table S1). The first pattern (hereafter referred to
224 as the 'increase'-group) included 48 viruses that increased in abundance from aposymbiotic to
225 partially populated and fully symbiotic Aiptasia (Fig. 2 A). This group was dominated by
226 *Herpesviridae* (7 species), *Baculoviridae* (5 species), and *Picornaviridae* (3 species). However,
227 only 13 of the 48 viral taxa assigned to this group were significantly differentially abundant,
228 including mainly viruses that are known to infect vertebrates (7 species) and invertebrates (3
229 species) (Supp. Table S2). Further, this group included a fungi-infecting species (*Penicillium*
230 *chrysogenum virus*), a plant-infecting species (*Bidens mottle virus*), as well as one plant- and
231 fungi-infecting viral species (*White clover cryptic virus* 2). The second pattern (hereafter
232 referred to as the 'decrease'-group) included 40 viral taxa that showed the opposite pattern: a
233 general decrease in relative abundance from aposymbiotic to partially populated and fully
234 symbiotic Aiptasia (Fig. 2 B) and were dominated by *Picornaviridae* (6 species), *Partitiviridae* (6
235 species), and *Bromoviridae* (3 species). However, none of the viral taxa were significantly
236 differentially abundant in this group (Supp. Table S2). The remaining viruses showed an
237 inconsistent pattern and were less frequent (28 viral taxa) (Supp. Table S2). Thus, the overall
238 viral community was rather consistent in terms of composition (Fig. 1) and abundance (Fig. 2),
239 although some viruses changed significantly in relative abundance in fully symbiotic animals,
240 but the functional significance of this remains to be determined.

241

242 *The Aiptasia core virome*

243 Despite the overall similarities in viral community compositions (Fig. 1) and abundance (Fig. 2),
244 we were interested to assess the viromes associated with aposymbiotic, partially populated,
245 and fully symbiotic Aiptasia. To do this, we determined all viral taxa that were 100% present in
246 all four replicates of the respective condition (i.e., aposymbiotic, partially populated, and fully
247 symbiotic). Partially populated Aiptasia anemones harbored the most diverse virome consisting
248 of 41 viral species, followed by the fully symbiotic (32 viral species), and aposymbiotic virome
249 (27 viral species) (Supp. Table S3). Thus, consistent with a significant increase in relative
250 abundance for some viral taxa in fully symbiotic anemones, we also found an overall increase in
251 viral diversity. Only few viral taxa were exclusively present in one of the symbiotic states and
252 the majority of viral taxa were present in more than one symbiotic state (Fig. 3). Further, a total
253 of 15 viral taxa across 11 families comprised the Aiptasia core virome (i.e., viral taxa present in
254 100% of all samples) (Fig. 3, Supp. Table S3). The Aiptasia core virome included the four most
255 abundant viral taxa and families, including viruses from the *Herpesviridae*, *Partitivirdae*, and
256 *Picornaviridae* families.

257

258

Discussion

Despite the importance of microorganisms to their multicellular hosts (McFall-Ngai et al., 2013), basic knowledge about the viral community of many organisms, including the model metaorganism Aiptasia, is still lacking. The vastness of next-generation sequencing datasets provides an opportunity to begin to investigate this microbial diversity, using approaches that filter the target organism and classify remaining sequence reads (Brüwer et al., 2017). In this study, we employed a previously generated Aiptasia RNA-Seq dataset to gain a first insight into the viral community associated with Aiptasia across three different symbiotic states (aposymbiotic, partially populated, fully symbiotic) with *Symbiodinium*. Of note, the here-assessed RNA-Seq libraries were oligodT-selected prior to library generations. Thus, a bias towards polyadenylated sequences is expected, putatively increasing our ability to detect ssRNA(+) viruses that contain polyadenylated viral genomes (Adams, Antoniw & Beaudoin, 2005; Le Gall et al., 2008), as well as dsDNA and ssRNA(+) viruses that polyadenylate their mRNAs (Majerciak et al., 2013; te Velthuis & Fodor, 2016). Our analysis, therefore, provides a first overview of the viral community, rather than a complete characterization.

Based on our analysis, Aiptasia CC7 anemones harbor a diverse viral community that appears to be similar in taxon richness compared to other non-stressed cnidarians, i.e. *Hydra* (Grasis et al., 2014). The assessed Aiptasia virome consists of 116 viral taxa from 40 viral families. Interestingly, almost all of the detected viral families have been described in corals (Wood-Charlson et al., 2015) or *Symbiodinium* (Brüwer et al., 2017). More specifically, 27 (in the case of corals) and 32 (in the case of *Symbiodinium*) out of 40 detected viral families in Aiptasia in this study were previously described. Firstly, this lends further support that our here-employed approach works and RNA-Seq data can be queried to gain a first insight into viral diversity. Secondly, it supports the notion that Aiptasia indeed is a suitable model of cnidarian-dinoflagellate symbiosis, not only at the level of host and algal symbiont biology (Baumgarten et al., 2015) but also at the level of bacteria (Röthig et al., 2016; Herrera et al., 2017) and viruses (this study).

The viral communities associated with Aiptasia are dominated by *Herpesviridae* (vertebrate-infecting), *Partitiviridae* (plant- and fungi -infecting), and *Picornaviridae* (vertebrate-infecting) (Hulo et al., 2011) (Fig. 1), which is of particular notice, given that Aiptasia is an invertebrate. However, vertebrate viruses have been frequently found in cnidarian viromes (Grasis et al., 2014; Wood-Charlson et al., 2015; Vega Thurber et al., 2017). A case study on the freshwater polyp *Hydra*, Grasis et al. (2014) suggested that the increased vertebrate-virus abundance might be due to a variety of ancestral genes that have been lost in other invertebrates, such as *Drosophila melanogaster* and *Caenorhabditis elegans*), as well as a great similarity of the genome organization. Despite these evolutionary considerations, caution has to be applied when categorizing viruses as vertebrate-, invertebrate-, or fungi-infection, etc. as this categorization is mainly based on previous findings and descriptions and might not have a claim to completeness. Last, the uneven presentation of viruses from different host organisms in viral databases might further contribute to uncertainties regarding these categorizations.

Despite our finding of an overall diverse and stable viral community associated with Aiptasia, we were interested to further assess whether the viral community is different under different symbiotic states (i.e., aposymbiotic, partially populated, and fully symbiotic). This would further contribute to our understanding of the intricacies of the cnidarian-dinoflagellate symbiosis (Mies et al., 2017) and provide putative important detail concerning the role of viruses in this symbiosis. We find that viral diversity and community composition remains overall stable, irrespective of the symbiotic state with *Symbiodinium minutum*. However, individual viral taxa change in abundance across symbiotic states. Most noticeably, we find significant abundance increases of 13 viral taxa when the host animal becomes partially populated and fully infected with *Symbiodinium* (Fig. 2 A). We initially hypothesized that members of the 'increase'-group would be dominated by plant-infecting viruses, given that *Symbiodinium* may come associated with its distinct set of viruses. However, we mainly observed vertebrate-infecting viruses, mostly *Herpesviridae*, as well as some invertebrate viruses to increase in abundance. In contrast to the 'increase'-group, the 'decrease'-group (Fig. 2 B) is comprised of viruses that decrease in abundance and is dominated by plant- and fungi-infecting viral species of the *Partitiviridae* family, as well as other plant-infecting viruses, such as

317 members of the *Virgaviridae* and *Bromoviridae* families, and vertebrate viruses, mainly of the
318 *Picornaiviridae* family. Notably, none of these changes were significant. As such, it remains to
319 be determined whether some viruses increase, whereas other viruses decrease upon entering
320 partially populated or fully symbiotic states. However, it is tempting to speculate that the viral
321 community might compensate and adapt to the changing environment, as suggested earlier for
322 the *Hydra* virome (Grasis et al., 2014).
323
324 To better understand the contribution of the virome to a metaorganism, knowledge about the
325 constantly associated viruses (i.e., viral taxa of the core virome) might provide further clues to
326 their importance and ecological significance. A case study in *Hydra* assessed the viral
327 community composition of four different *Hydra* strains and concluded that the virome, similar
328 to the microbiome, is species-specific (Grasis et al., 2014). Presuming a similar pattern for
329 Aiptasia, we aimed to identify permanent members of the viral community. In our study,
330 viruses that were present in all samples were considered members of the core virome and,
331 thus, suggested to be permanent members of the viral community. Interestingly, plant- and
332 vertebrate-infecting viruses dominate the here-identified Aiptasia core virome.
333 The Aiptasia core virome comprises 15 viral species from 11 viral families, which is in
334 line with a recent review by Vega Thurber et al. (2017) proposing between 9 and 12 viral
335 families as members of a coral core virome. More specifically, viruses of the *Mimivirdae*,
336 *Herpesviridae*, and *Poxviridae* families were suggested to be part of the coral core virome (Vega
337 Thurber et al., 2017) and are also present in the Aiptasia core virome. In addition, viruses
338 similar to the *Herpesviridae* family have been described in almost all studies investigating the
339 viral community of anthozoans (Grasis et al., 2014; Wood-Charlson et al., 2015; Vega Thurber et
340 al., 2017) including this study, and thus, are most likely important members of the cnidarians
341 metaorganism. Bacteriophages of the order Caudovirales (including *Siphoviridae, Podoviridae*,
342 and *Myoviridae*), which are most abundant members of the *Hydra* virome (Grasis et al., 2014)
343 and are frequently present in coral viromes (Wood-Charlson et al., 2015), were, however,
344 absent in the Aiptasia core virome. Taken together, despite some differences to other
345 anthozoan viromes, which may be partially attributed to a bias stemming from our approach to

use RNA-Seq data, the Aiptasia viral community exhibits a comparable complexity and harbors a large similarity in composition compared to anthozoan core viromes. Henceforth, our analyses support Aiptasia as a model metaorganism to study not only the cnidarian-dinoflagellate symbiosis but also the role of associated viruses with potential implications for coral health.

Conclusions

Although the power and validity of the metaorganism concept receive growing attention, we know little about the viral communities associated with many animals and host, in particular of corals and other marine invertebrates. To further complement the usability and resources available for the Aiptasia model system, we annotated RNA-Seq data to describe the virome associated with aposymbiotic, partially populated, and fully symbiotic Aiptasia. We find that Aiptasia is associated with a diverse and stable viral community. Certain viral taxa of this community increase their abundance when aposymbiotic anemones establish a symbiotic relationship with their endosymbiont *Symbiodinium*. Hence, the viral community responds to the symbiosis suggesting putative functional implications that need to be assessed in future studies. Further, we identified candidate members of the Aiptasia core virome comprised of viruses from the families *Mimiviridae*, *Heperesviridae*, and *Poxviridae* families that resembles the composition of coral core viromes. The Aiptasia model metaorganism may facilitate targeted studies to investigate the ecological importance of viruses the cnidarian-dinoflagellate endosymbiosis with implications for coral reef health.

Acknowledgements

JDB was funded by a Visiting Student Research Program (VSRP) fellowship awarded by King Abdullah University of Science and Technology (KAUST). Additional supported was provided by baseline funds from KAUST to CRV. The funders had no role in the design of the study and collection, analysis, and interpretation of data, and in writing the manuscript.

Author contribution

JDB and CRV designed and conceived the study. JDB generated data. JDB and CRV analyzed data. JDB and CRV wrote the manuscript.

List of abbreviations

AFSW	sterile-filtered artificial sea-water
bp	base pairs
ChocGV	*Choristoneura occidentalis granulovirus*
dsDNA	double-stranded DNA virus
dsRNA	double-stranded RNA virus
RNA-Seq	RNA-sequencing
rRNA	ribosomal RNA
ssRNA(+)	positive-sense single-stranded RNA virus
ssRNA(-)	negative-sense single-stranded RNA virus
ssRNA(rt)	reverse-transcribing single-stranded RNA virus

References

Adams MJ., Antoniw JF., Beaudoin F. 2005. Overview and analysis of the polyprotein cleavage sites in the family Potyviridae. *Molecular Plant Pathology* 6:471–487. DOI: 10.1111/j.1364-3703.2005.00296.x.

Aronesty E. 2011. ea-utils: Command-line tools for processing biological sequencing data. *Expression Analysis, Durham, NC*.

Baumgarten S., Simakov O., Esherick LY., Liew YJ., Lehnert EM., Michell CT., Li Y., Hambleton EA., Guse A., Oates ME., Gough J., Weis VM., Aranda M., Pringle JR., Voolstra CR. 2015. The genome of Aiptasia, a sea anemone model for coral symbiosis. *Proceedings of the National Academy of Sciences of the United States of America* 112:11893–11898. DOI: 10.1073/pnas.1513318112.

Bolger AM., Lohse M., Usadel B. 2014. Trimmomatic: A flexible trimmer for Illumina sequence data. *Bioinformatics* 30:2114–2120. DOI: 10.1093/bioinformatics/btu170.

Bosch TCG., McFall-Ngai MJ. 2011. Metaorganisms as the new frontier. *Zoology* 114:185–190. DOI: 10.1016/j.zool.2011.04.001.

Brüwer JD., Agrawal S., Liew YJ., Aranda M., Voolstra CR. 2017. Association of coral algal symbionts with a diverse viral community responsive to heat shock. *BMC Microbiology* 17:174. DOI: 10.1186/s12866-017-1084-5.

Bushnell B. 2016. BBMap short read aligner. *University of California, Berkeley, California. URL http://sourceforge. net/projects/bbmap*.

Correa AMS., Ainsworth TD., Rosales SM., Thurber AR., Butler CR., Vega Thurber RL. 2016. Viral outbreak in corals associated with an in situ bleaching event: Atypical herpes-like viruses and a new megavirus infecting symbiodinium. *Frontiers in Microbiology* 7:1–14. DOI: 10.3389/fmicb.2016.00127.

Davison AJ. 2017. Journal of general virology - Introduction to “ICTV virus taxonomy profiles.” *Journal of General Virology* 98:1. DOI: 10.1099/jgv.0.000686.

Falkowski PG., Dubinsky Z., Muscatine L., Porter JW. 1984. Light and the Bioenergetics of a Symbiotic Coral. *Source: BioScience* 34:705–709.

Le Gall O., Christian P., Fauquet CM., King AMQ., Knowles NJ., Nakashima N., Stanway G.,

Gorbalenya AE. 2008. Picornavirales, a proposed order of positive-sense single-stranded RNA viruses with a pseudo-T = 3 virion architecture. *Archives of Virology* 153:715–727. DOI: 10.1007/s00705-008-0041-x.

Gentleman R., Carey V., Bates D., Bolstad B., Dettling M., Dudoit S., Ellis B., Gautier L., Ge Y., Gentry J., Hornik K., Hothorn T., Huber W., Iacus S., Irizarry R., Leisch F., Li C., Maechler M., Rossini A., Sawitzki G., Smith C., Smyth G., Tierney L., Yang J., Zhang J. 2004. Bioconductor: open software development for computational biology and bioinformatics. *Genome Biology* 5:R80. DOI: 10.1186/gb-2004-5-10-r80.

Grasis JA., Lachnit T., Anton-Erxleben F., Lim YW., Schmieder R., Fraune S., Franzenburg S., Insua S., Machado G., Haynes M., Little M., Kimble R., Rosenstiel P., Rohwer FL., Bosch TCG. 2014. Species-specific viromes in the ancestral holobiont hydra. *PLoS ONE* 9:e109952. DOI: 10.1371/journal.pone.0109952.

Hambleton EA., Guse A., Pringle JR. 2014. Similar specificities of symbiont uptake by adults and larvae in an anemone model system for coral biology. *The Journal of Experimental Biology* 217:1613–1619. DOI: 10.1242/jeb.095679.

Herrera M., Ziegler M., Voolstra CR., Aranda Lastra MI. 2017. Laboratory-cultured strains of the sea anemone *Exaiptasia* reveal distinct bacterial communities. *Frontiers in Marine Science* 4:115.

Hoegh-Guldberg O. 1999. Climate Change, coral bleaching and the future of the world's coral reef. *CSIRO Australia* 50:839–66. DOI: 10.1071/MF00030.

Hughes TP., Baird AH., Bellwood DR., Card M., Connolly SR., Folke C., Grosberg R., Hoegh-Guldberg O., Jackson JBC., Kleypas J. 2003. Climate change, human impacts, and the resilience of coral reefs. *Science* 301:929–933. DOI: 10.1126/science.1085046.

Hughes TP., Kerry JT., Álvarez-Noriega M., Álvarez-Romero JG., Anderson KD., Baird AH., Babcock RC., Beger M., Bellwood DR., Berkelmans R. 2017. Global warming and recurrent mass bleaching of corals. *Nature* 543:373–377. DOI: 10.1038/nature21707.

Hulo C., De Castro E., Masson P., Bougueleret L., Bairoch A., Xenarios I., Le Mercier P. 2011. ViralZone: a knowledge resource to understand virus diversity. *Nucleic Acids Research* 39:D576–D582.

448 Hulsen T., de Vlieg J., Alkema W. 2008. BioVenn – a web application for the comparison and
449 visualization of biological lists using area-proportional Venn diagrams. *BMC Genomics*
450 9:488. DOI: 10.1186/1471-2164-9-488.
451 Hurlbert SH. 1971. The nonconcept of species diversity: a critique and alternative parameters.
452 *Ecology* 52:577–586. DOI: 10.2307/1934145.
453 IPCC. 2014. *Climate change 2014: synthesis report. Contribution of Working Groups I, II and III to*
454 *the fifth assessment report of the Intergovernmental Panel on Climate Change*.
455 Knowlton N., Rohwer F. 2003. Multispecies microbial mutualisms on coral reefs: the host as a
456 habitat. *the american naturalist* 162:S51–S62. DOI: doi.org/10.1086/378684.
457 Lesser MP., Jarett JK. 2014. Culture-dependent and culture-independent analyses reveal no
458 prokaryotic community shifts or recovery of Serratia marcescens in *Acropora palmata* with
459 white pox disease. *FEMS Microbiology Ecology* 88:457–467. DOI: 10.1111/1574-
460 6941.12311.
461 Levin RA., Voolstra CR., Weynberg KD., van Oppen MJH. 2016. Evidence for a role of viruses in
462 the thermal sensitivity of coral photosymbionts. *The ISME Journal* 11:808–812. DOI:
463 10.1038/ismej.2016.154.
464 Liew YJ., Aranda M., Voolstra CR. 2016. Reefgenomics. Org-a repository for marine genomics
465 data. *Database* 2016:baw152.
466 Majerciak V., Ni T., Yang W., Meng B., Zhu J., Zheng ZM. 2013. A Viral Genome Landscape of
467 RNA Polyadenylation from KSHV Latent to Lytic Infection. *PLoS Pathogens* 9:e1003749.
468 DOI: 10.1371/journal.ppat.1003749.
469 Marhaver KL., Edwards RA., Rohwer F. 2008. Viral communities associated with healthy and
470 bleaching corals. *Environmental Microbiology* 10:2277–2286. DOI: 10.1111/j.1462-
471 2920.2008.01652.x.
472 McFall-Ngai M., Hadfield MG., Bosch TCG., Carey H V., Domazet-Lošo T., Douglas AE., Dubilier
473 N., Eberl G., Fukami T., Gilbert SF., Hentschel U., King N., Kjelleberg S., Knoll AH., Kremer
474 N., Mazmanian SK., Metcalf JL., Nealson K., Pierce NE., Rawls JF., Reid A., Ruby EG.,
475 Rumpho M., Sanders JG., Tautz D., Wernegreen JJ. 2013. Animals in a bacterial world, a
476 new imperative for the life sciences. *Proceedings of the National Academy of Sciences*

110:3229–3236. DOI: 10.1073/pnas.1218525110.

Mies M., Sumida PYG., Rädecker N., Voolstra CR. 2017. Marine Invertebrate Larvae Associated with Symbiodinium: A Mutualism from the Start? *Frontiers in Ecology and Evolution* 5:1–11. DOI: 10.3389/fevo.2017.00056.

Muscatine L. 1967. Glycerol Excretion by symbiotic algae from corals and tridacna and its control by the host. *Science* 156:516–519. DOI: 10.1126/science.156.3774.516.

Muscatine L., Porter JW. 1977. Reef corals: mutualistic symbioses adapted to nutrient-poor environments. *Bioscience* 27:454–460. DOI: doi.org/10.2307/1297526.

Oksanen J., Blanchet FG., Friendly M., Kindt R., Legendre P., McGlinn D., Minchin PR., O'Hara RB., Simpson GL., Solymos P., Henry M., Stevens H., Szoecs E., Wagner H. 2017. Vegan: Community Ecology Package. 2017. R-package version 2.4-2.

Ounit R., Wanamaker S., Close TJ., Lonardi S. 2015. CLARK: fast and accurate classification of metagenomic and genomic sequences using discriminative k-mers. *BMC Genomics* 16:236. DOI: 10.1186/s12864-015-1419-2.

Paulson J. 2014. metagenomeSeq: Statistical analysis for sparse high-throughput sequencing. *Bioconductor.Jp*:1–20.

Paulson JN., Stine OC., Bravo HC., Pop M. 2013. Differential abundance analysis for microbial marker-gene surveys. *Nature Methods* 10:1200–2. DOI: 10.1038/nmeth.2658.

R Core Team. 2016. R: A language and environment for statistical computing. Vienna: R Foundation for Statistical Computing, Vienna, Austria.

Rädecker N., Pogoreutz C., Voolstra CR., Wiedenmann J., Wild C. 2015. Nitrogen cycling in corals: The key to understanding holobiont functioning? *Trends in Microbiology* 23:490–497. DOI: 10.1016/j.tim.2015.03.008.

Rohwer F., Seguritan V., Azam F., Knowlton N. 2002. Diversity and distribution of coral-associated bacteria. *Marine Ecology Progress Series* 243:1–10. DOI: 10.3354/meps243001.

Rosenberg E., Koren O., Reshef L., Efrony R., Zilber-Rosenberg I. 2007. The role of microorganisms in coral health, disease and evolution. *Nature Reviews Microbiology* 5:355–362. DOI: 10.1038/nrmicro1635.

Röthig T., Costa RM., Simona F., Baumgarten S., Torres AF., Radhakrishnan A., Aranda M.,

Voolstra CR. 2016. Distinct Bacterial Communities Associated with the Coral Model *Aiptasia* in Aposymbiotic and Symbiotic States with *Symbiodinium*. *Frontiers in Marine Science* 3:234. DOI: 10.3389/fmars.2016.00234.

Shoguchi E., Shinzato C., Kawashima T., Gyoja F., Mungpakdee S., Koyanagi R., Takeuchi T., Hisata K., Tanaka M., Fujiwara M. 2013. Draft assembly of the *Symbiodinium minutum* nuclear genome reveals dinoflagellate gene structure. *Current biology* 23:1399–1408.

Soffer N., Brandt ME., Correa AMS., Smith TB., Thurber RV. 2014. Potential role of viruses in white plague coral disease. *The ISME Journal* 8:271–283. DOI: 10.1038/ismej.2013.137.

Thornhill DJ., Xiang Y., Pettay DT., Zhong M., Santos SR. 2013. Population genetic data of a model symbiotic cnidarian system reveal remarkable symbiotic specificity and vectored introductions across ocean basins. *Molecular Ecology* 22:4499–4515. DOI: 10.1111/mec.12416.

Torda G., Donelson JM., Aranda M., Barshis DJ., Bay L., Berumen ML., Bourne DG., Cantin N., Foret S., Matz M. 2017. Rapid adaptive responses to climate change in corals. *Nature Climate Change* 7:627–636. DOI: 10.1038/NCLIMATE3374.

Vega Thurber R., Payet JP., Thurber AR., Correa AMS. 2017. Virus–host interactions and their roles in coral reef health and disease. *Nature Reviews Microbiology* 15:205–216. DOI: 10.1038/nrmicro.2016.176.

te Velthuis AJW., Fodor E. 2016. Influenza virus RNA polymerase: insights into the mechanisms of viral RNA synthesis. *Nature Reviews Microbiology* 14:479–493. DOI: 10.1038/nrmicro.2016.87.

Voolstra CR. 2013. A journey into the wild of the cnidarian model system Aiptasia and its symbionts. *Molecular Ecology* 22:4366–4368. DOI: 10.1111/mec.12464.

Weis VM., Davy SK., Hoegh-Guldberg O., Rodriguez-Lanetty M., Pringle JR. 2008. Cell biology in model systems as the key to understanding corals. *Trends in Ecology and Evolution* 23:369–376. DOI: doi.org/10.1016/j.tree.2008.03.004.

Weynberg KD., Levin RA., Neave MJ., Clode PL., Voolstra CR., Brownlee C., Laffy PW., Webster NS., Wood-charlson EM., Oppen JH Van., Biology PF., Cluster CC., Sea R., Science E., Arabia S., Resources B. 2017. Prevalent viral infection in cultures of the coral algal endosymbiont

Symbiodinium. *Coral Reefs* 36:773–784. DOI: 10.1007/s00338-017-1568-7.

Weynberg KD., Voolstra CR., Neave MJ., Buerger P., van Oppen MJH. 2015. From cholera to corals: Viruses as drivers of virulence in a major coral bacterial pathogen. *Scientific Reports* 5:17889. DOI: 10.1038/srep17889.

Wickham H. 2016. *ggplot2: elegant graphics for data analysis*. Cham: Springer.

Wolfowicz I., Baumgarten S., Voss PA., Hambleton EA., Voolstra CR., Hatta M., Guse A. 2016. *Aiptasia sp.* larvae as a model to reveal mechanisms of symbiont selection in cnidarians. *Scientific Reports* 6:32366. DOI: 10.1038/srep32366.

Wood-Charlson EM., Weynberg KD., Suttle C a., Roux S., van Oppen MJH. 2015. Metagenomic characterisation of viral communities in corals: Mining biological signal from methodological noise. *Environmental Microbiology* 17:1–21. DOI: 10.1111/1462-2920.12803.

Xiang T., Hambleton EA., Denofrio JC., Pringle JR., Grossman AR. 2013. Isolation of clonal axenic strains of the symbiotic dinoflagellate *Symbiodinium* and their growth and host specificity1. *Journal of Phycology* 49:447–458. DOI: 10.1111/jpy.12055.

Ziegler M., Seneca FO., Yum LK., Palumbi SR., Voolstra CR. 2017. Bacterial community dynamics are linked to patterns of coral heat tolerance. *Nature Communications* 8:14213. DOI: 10.1038/ncomms14213.

554 **Tables**

555

556 **Table 1. Sequence data overview and read-based annotation.** Numbers of raw and retained
557 (i.e., after quality filtering, trimming, and removal of host anemones, symbiont algae, PhiX, 28S
558 rRNA) sequence reads, as well as number of annotated read pairs are provided. Retained
559 sequence reads were used for taxonomic analysis. Apo = aposymbiotic; Partial = partially
560 populated (after 12 days of infection); Symbiotic = fully symbiotic (fully infected, after 30 days
561 of infection). R1 – R4 = replicated anemones.

562

563 **Table 2. Overview of Aiptasia viral community richness, evenness, diversity, and most**
564 **abundant viral taxon.** Species richness was estimated following Hurlbert (1971) after rarefying
565 to the lowest number of viral-annotated sequences (n = 82). Apo = aposymbiotic; Partial =
566 partially populated (after 12 days of infection); Symbiotic = fully symbiotic (fully infected, after
567 30 days of infection). R1 – R4 = replicated anemones.

568

Figures

Figure 1. Aiptasia viral community composition. Shown are the 10 most abundant viral families associated with adult Aiptasia anemones across three symbiotic stages (aposymbiotic, partially populated, and fully symbiotic); remaining viruses are associated under 'Others'. Apo = aposymbiotic; Partially = partially populated (after 12 days of infection); Sym = fully symbiotic (fully infected, after 30 days of infection). 1 – 4 = replicated anemones.

Figure 2. Relative abundance changes of viruses associated with Aiptasia in relation to aposymbiotic, partially populated, and fully symbiotic anemones. Viral taxa could be separated into two groups: (A) viral taxa that increased in abundance from aposymbiotic to partially populated and fully symbiotic Aiptasia ('increase' group); (B) viral taxa that showed a general decrease in abundance from aposymbiotic to partially populated and fully symbiotic Aiptasia.

Figure 3. Viromes associated with aposymbiotic, partially populated, and fully symbiotic Aiptasia. All viral taxa present in 100% across all four replicates of the respective state (i.e., aposymbiotic (red area), partially populated (yellow area), and fully symbiotic (blue area)) were considered virome members. The core virome (dark gray area) denotes the intersection of viromes from aposymbiotic, partially populated, and fully symbiotic anemones: 15 viral taxa were present in 100% of all samples and are proposed members of the Aiptasia core virome. The areas correspond proportionally to the number of viral taxa they encompass.

Supplementary Information

Supp. Table S1. CSS normalized sequence counts for all annotated viruses. The viral spreadsheet is completed with genome organization information and information about respective hosts. A1M – A4M: aposymbiotic; I1M – I4M = partially populated (after 12 days of infection); S1M – S4M = fully symbiotic (fully infected, after 30 days of infection).

Supp. Table S2. Abundance changes of viruses associated with Aiptasia in relation to aposymbiotic, partially populated, and fully symbiotic anemones. Shown are viral taxa tested, ANOVA p-values (significant values in bold), and associated post-hoc Tukey tests, as well as assortment to the 'increase' and 'decrease' group.

Supp. Table S3. Aiptasia core virome and viromes associated with aposymbiotic, partially populated, and fully symbiotic anemones of Aiptasia. Only viruses present in 100% of each respective symbiotic state were considered. Viruses present across all samples comprise the core virome. Members of the core virome are highlighted in bold.

Supp. Data Sheet S1. List of bioinformatics software and commands used.

Supp. Figure S1. Overview of bioinformatics pipeline.

Table 1 (on next page)

Table 1. Sequence data overview and read-based annotation.

Table 1. Sequence data overview and read-based annotation. Numbers of raw and retained (i.e., after quality filtering, trimming, and removal of host anemones, symbiont algae, PhiX, 28S rRNA) sequence reads, as well as number of annotated read pairs are provided. Retained sequence reads were used for taxonomic analysis. Apo = aposymbiotic; Partial = partially populated (after 12 days of infection); Symbiotic = fully symbiotic (fully infected, after 30 days of infection). R1 – R4 = replicated anemones.

Condition	Sample	Raw reads	Retained reads	Classified read pairs (total)	Classified read pairs (virus)	Classified read pairs (bacteria)	Classified read pairs (archaea)
Apo	R1	23,314,626	633,310	2,220	82	2,136	2
	R2	21,623,164	640,332	2,176	203	1,965	8
	R3	23,905,820	702,856	3,413	199	3,206	8
	R4	23,200,990	803,114	8,407	552	7,840	15
Partial	R1	21,485,094	798,846	8,752	733	7,980	39
	R2	23,355,938	657,924	2,215	232	1,973	10
	R3	26,458,678	665,100	2,318	207	2,099	12
	R4	33,532,640	818,942	2,743	277	2,452	14
Symbiotic	R1	23,292,594	653,802	1,172	171	996	5
	R2	25,013,812	684,102	1,516	220	1,286	10
	R3	24,218,018	704,760	1,284	165	1,112	7
	R4	27,806,330	834,516	1,874	252	1,604	18
Total		297,207,704	8,597,604	38,090	3,293	34,649	148
Percentage					8.65%	90.97%	0.39%

Table 2 (on next page)

Table 2. Overview of Aiptasia viral community richness, evenness, diversity, and most abundant viral taxon.

Table 2. Overview of Aiptasia viral community richness, evenness, diversity, and most abundant viral taxon. Species richness was estimated following Hurlbert (1971) after rarefying to the lowest number of viral-annotated sequences (n = 82). Apo = aposymbiotic; Partial = partially populated (after 12 days of infection); Symbiotic = fully symbiotic (fully infected, after 30 days of infection). R1 – R4 = replicated anemones.

Condition	Replicate	Species richness (Hurlbert)	Evenness (Pielou)	Shannon-Wiener Diversity Index	Most abundant viral taxon
Apo	R1	29.264	0.911	3.312	15.85%
	R2	36.623	0.908	3.749	8.37%
	R3	37.751	0.914	3.803	8.04%
	R4	36.821	0.863	3.792	7.07%
Partial	R1	35.387	0.853	3.727	9.41%
	R2	35.039	0.890	3.660	10.78%
	R3	39.679	0.921	3.900	7.73%
	R4	39.386	0.901	3.902	7.22%
Symbiotic	R1	34.496	0.877	3.606	10.53%
	R2	37.559	0.903	3.784	10.00%
	R3	38.547	0.905	3.820	10.91%
	R4	40.108	0.904	3.915	8.73%

Figure 1 (on next page)

Figure 1. Aiptasia viral community composition.

Shown are the 10 most abundant viral families associated with adult Aiptasia anemones across three symbiotic stages (aposymbiotic, partially populated, and fully symbiotic); remaining viruses are associated under ‘Others’. Apo = aposymbiotic; Partially = partially populated (after 12 days of infection); Sym = fully symbiotic (fully infected, after 30 days of infection). 1 – 4 = replicated anemones.

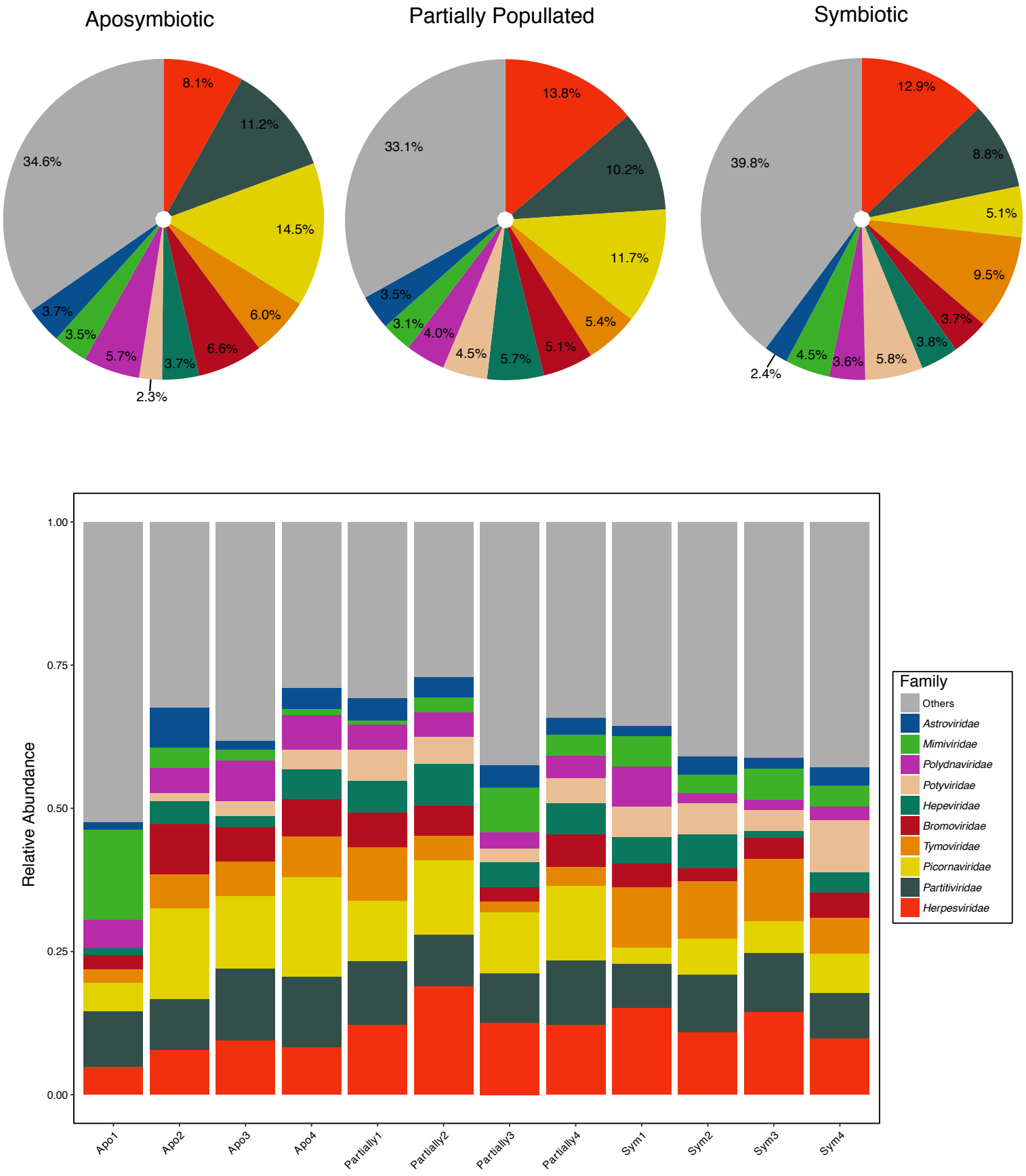
Aposymbiotic
8.1%
11.2%
34.6%
14.5%
3.7%
6.0%
3.5%
5.7%
6.6%
3.7%
2.3%
Partially Popullated
13.8%
33.1%
10.2%
11.7%
3.5%
5.4%
3.1%
4.0%
5.1%
4.5%
5.7%
Symbiotic
12.9%
8.8%
39.8%
5.1%
9.5%
3.7%
3.8%
4.5%
3.6%
5.8%
2.4%
Relative Abundance
1.00
0.75
0.50
0.25
0.00
Apo1
Apo2
Apo3
Apo4
Partially1
Partially2
Partially3
Partially4
Sym1
Sym2
Sym3
Sym4
Family
Others
Astroviridae
Mimiviridae
Polydnaviridae
Potyviridae
Hepeviridae
Bromoviridae
Tymoviridae
Picornaviridae
Partitiviridae
Herpesviridae

Figure 2 (on next page)

Figure 2. Relative abundance changes of viruses associated with Aiptasia in relation to aposymbiotic, partially populated, and fully symbiotic anemones.

Viral taxa could be separated into two groups: (A) viral taxa that increased in abundance from aposymbiotic to partially populated and fully symbiotic Aiptasia (‘increase’ group); (B) viral taxa that showed a general decrease in abundance from aposymbiotic to partially populated and fully symbiotic Aiptasia.

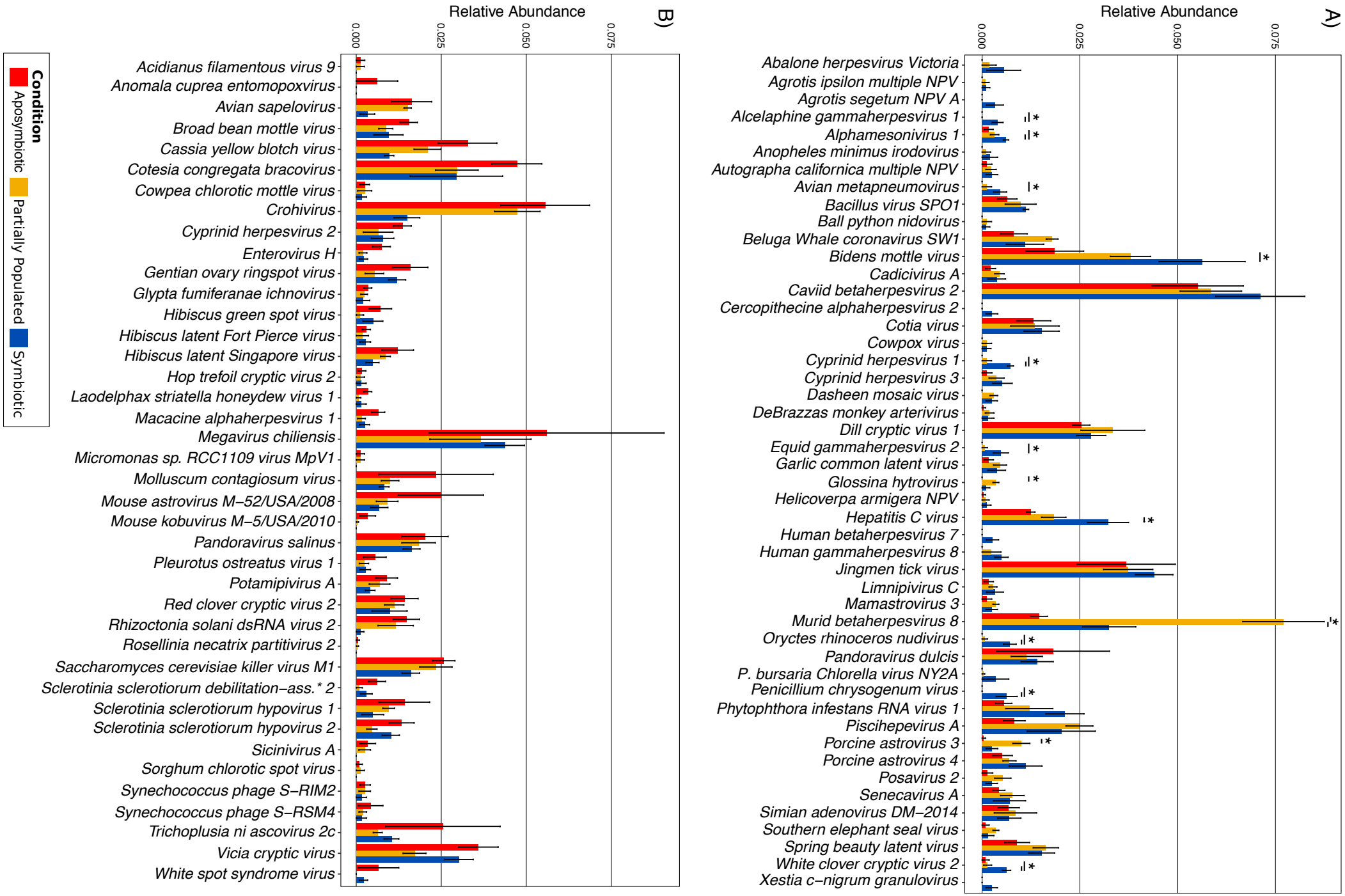
A)
Relative Abundance
0.000
0.025
0.050
0.075
Abalone herpesvirus Victoria
Agrotis ipsilon multiple NPV
Agrotis segetum NPV A
Alcelaphine gammaherpesvirus 1
Alphamesonivirus 1
Anopheles minimus irodovirus
Autographa californica multiple NPV
Avian metapneumovirus
Bacillus virus SPO1
Ball python nidovirus
Beluga Whale coronavirus SW1
Bidens mottle virus
Cadicivirus A
Caviid betaherpesvirus 2
Cercopithecine alphaherpesvirus 2
Cotia virus
Cowpox virus
Cyprinid herpesvirus 1
Cyprinid herpesvirus 3
Dasheen mosaic virus
DeBrazzas monkey arterivirus
Dill cryptic virus 1
Equid gammaherpesvirus 2
Garlic common latent virus
Glossina hytrovirus
Helicoverpa armigera NPV
Hepatitis C virus
Human betaherpesvirus 7
Human gammaherpesvirus 8
Jingmen tick virus
Limnipivirus C
Mamastrovirus 3
Murid betaherpesvirus 8
Oryctes rhinoceros nudivirus
Pandoravirus dulcis
P. bursaria Chlorella virus NY2A
Penicillium chrysogenum virus
Phytophthora infestans RNA virus 1
Piscihepevirus A
Porcine astrovirus 3
Porcine astrovirus 4
Posavirus 2
Senecavirus A
Simian adenovirus DM–2014
Southern elephant seal virus
Spring beauty latent virus
White clover cryptic virus 2
Xestia c–nigrum granulovirus
B)
Relative Abundance
0.000
0.025
0.050
0.075
Acidianus filamentous virus 9
Anomala cuprea entomopoxvirus
Avian sapelovirus
Broad bean mottle virus
Cassia yellow blotch virus
Cotesia congregata bracovirus
Cowpea chlorotic mottle virus
Crohivirus
Cyprinid herpesvirus 2
Enterovirus H
Gentian ovary ringspot virus
Glypta fumiferanae ichnovirus
Hibiscus green spot virus
Hibiscus latent Fort Pierce virus
Hibiscus latent Singapore virus
Hop trefoil cryptic virus 2
Laodelphax striatella honeydew virus 1
Macacine alphaherpesvirus 1
Megavirus chiliensis
Micromonas sp. RCC1109 virus MpV1
Molluscum contagiosum virus
Mouse astrovirus M–52/USA/2008
Mouse kobuvirus M–5/USA/2010
Pandoravirus salinus
Pleurotus ostreatus virus 1
Potamipivirus A
Red clover cryptic virus 2
Rhizoctonia solani dsRNA virus 2
Rosellinia necatrix partitivirus 2
Saccharomyces cerevisiae killer virus M1
Sclerotinia sclerotiorum debilitation–ass.* 2
Sclerotinia sclerotiorum hypovirus 1
Sclerotinia sclerotiorum hypovirus 2
Sicinivirus A
Sorghum chlorotic spot virus
Synechococcus phage S–RIM2
Synechococcus phage S–RSM4
Trichoplusia ni ascovirus 2c
Vicia cryptic virus
White spot syndrome virus
Condition
Aposymbiotic
Partially Populated
Symbiotic

Figure 3 (on next page)

Figure 3. Viromes associated with aposymbiotic, partially populated, and fully symbiotic Aiptasia.

All viral taxa present in 100% across all four replicates of the respective state (i.e., aposymbiotic (red area), partially populated (yellow area), and fully symbiotic (blue area)) were considered virome members. The core virome (dark gray area) denotes the intersection of viromes from aposymbiotic, partially populated, and fully symbiotic anemones: 15 viral taxa were present in 100% of all samples and are proposed members of the Aiptasia core virome. The areas correspond proportionally to the number of viral taxa they encompass.

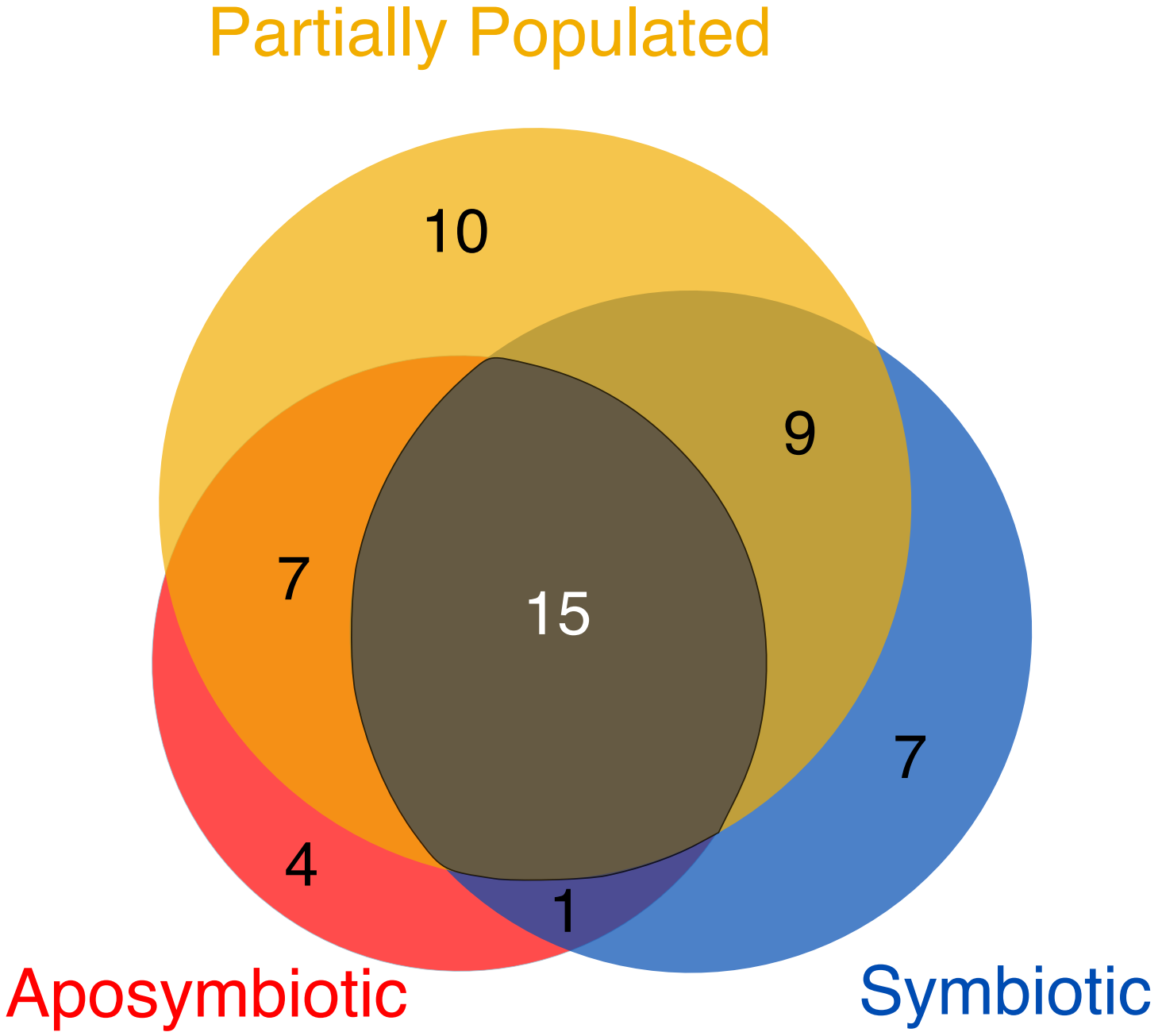
Partially Populated
10
9
7
15
7
4
1
Aposymbiotic
Symbiotic